The Mathematical Model of Bearingless Switched Reluctance Motors With Two-Phase Excitation

Cao Xin, Deng Zhiquan, Yang Gang, and Wang Xiaolin

Department of Electrical Engineering
Nanjing University of Aeronautics & Astronautics
Nanjing 210016,China
cxxc118@nuaa.edu.cn

Abstract **– In view of limitations of mathematical model only suited for the single-phase excitation mode in bearingless switched reluctance motors (BSRM), a novel mathematical model of BSRM with one or two-phase excitation is proposed. The inductance matrix is constructed based on the magnetic equivalent circuits in the two-phase excitation mode. New mathematical formulas of radial force and electromagnetic torque are derived. The operating area of BSRM can be expanded to a great extent. The capability of bearing radial force is enhanced greatly. Computer simulations with magnetic-field analytical-method verify the validity and fine characteristics of the new mathematical model. Two optimizing methods to distribute currents of two-phase windings including main windings and radial force windings for practical applications are also proposed.**

Index Terms **– Bearingless switched reluctance motor, mathematical model, two-phase excitation**

I. Introduction

Recently, various bearingless motors have been proposed. They combine the characteristics of typical motors and magnetic bearings. Bearingless motors have superior possibilities such as dense configuration, convenient maintenance, low cost, and miniaturization. The bearingless motor can break through the restriction of large power and super-speed, because its axial length decreases greatly and its inherent stiffness increases accordingly. So the application of switched reluctance motors (SRM) is broadened.

Switched reluctance motors have nice possibilities as bearingless motors. In principle, torque is generated by the magnetic attraction between stator and rotor poles. In this process, significant radial forces are generated which are bringing on noise and vibration in switched reluctance motors. Bearingless switched reluctance motors (BSRM) take advantage of these large radial forces to suspend the rotor [1]-[6]. And it also provides a new approach to solve the problems of SRM's noise and vibration.

The mathematical model suited for the single-phase excitation mode is introduced in 12/8 BSRM. As the rotor deviating from the stator, the radial force produced in the motor becomes very small. In bearingless switched reluctance generator, the currents of freewheeling phase and excitation phase could be overlap or discontinuous due to that the current of main winding can't be controlled in the freewheeling phase. The traditional control method of BSRM using square-wave currents should not be used.

In the implemented hardware system of BSRM, the topology of three-phase half-bridge converter is applied in the radial force winding. The middle voltage of two capacitors swings because of the asymmetry of loads. And the increase of radial force winding currents aggravates the middle voltage's excursion. In a certain extent, this could make the motor suspend unsteadily. If the two-phase excitation mode in BSRM was introduced, this problem will be avoidable by making the two middle capacitors charge or discharge alternately.

With respect to the limitation of the single-phase excitation mode, the two-phase excitation mode is proposed in BSRM. This paper firstly demonstrates the modeling procedure based on two-phase excitation mode. Then radial forces and the electromagnetic torque are derived. The FEM results validate the novel mathematical model of BSRM with two-phase excitation. The operating area of BSRM and the comparison of the traditional mathematical model and the novel mathematical model are proposed. Two optimizing methods to distribute currents of two-phase windings including main windings and radial force windings for practical applications are also illustrated in this paper.

II. TWO-PHASE EXCITATION MODE

A. Magnetic Equivalent Circuits

Fig. 1(a) shows a 12/8 BSRM superimposed by a magnetic equivalent circuit and each phase winding configuration. Where, Voltage source is “ ”. And permeances of air-gap are expressed as “ ”. Due to that the mutual inductance between each two-phase windings is small, the model of BSRM based on any two phases are analyzed when two phases excited in main windings. The parameters in Fig. 1 are as follows.

N_m—— the number of turns of the main winding

N_b—— the number of turns of the radial force winding

i_{ma}, i_{mb}—— the currents of phase A and B respectively

i_{sa1}, i_{sa2}, i_{sb1}, and i_{sb2}—— the currents of radial force windings of phase A and B in α and β axis

* This work is supported by National Natural Science Foundation of China(NSFC)(50377012).

$P_{a1} \sim P_{a4}$, $P_{b1} \sim P_{b4}$—— the air permeances of each pole in phase A and B

$\varphi_{a1} \sim \varphi_{a4}$, $\varphi_{b1} \sim \varphi_{b4}$—— the air fluxes of each pole in phase A and B

Equations (1)~(7) are derived from Fig. 1(b), according to the theory of that a sum of magnetomotive forces in each branch is equal to another one.

$$\frac{\phi_{a2}}{P_{a2}} - N_m i_{ma} + N_b i_{sa2} = \frac{\phi_{a1}}{P_{a1}} + N_m i_{ma} + N_b i_{a1} \tag{1}$$

$$\frac{\phi_{a3}}{P_{a3}} + N_m i_{ma} - N_b i_{sa1} = \frac{\phi_{a1}}{P_{a1}} + N_m i_{ma} + N_b i_{a1} \tag{2}$$

$$\frac{\phi_{a4}}{P_{a4}} - N_m i_{ma} - N_b i_{sa2} = \frac{\phi_{a1}}{P_{a1}} + N_m i_{ma} + N_b i_{a1} \tag{3}$$

$$\frac{\phi_{b1}}{P_{b1}} + N_m i_{mb} - N_b i_{sb1} = \frac{\phi_{a1}}{P_{a1}} + N_m i_{ma} + N_b i_{a1} \tag{4}$$

$$\frac{\phi_{b2}}{P_{b2}} - N_m i_{mb} + N_b i_{sb2} = \frac{\phi_{a1}}{P_{a1}} + N_m i_{ma} + N_b i_{a1} \tag{5}$$

$$\frac{\phi_{b3}}{P_{b3}} + N_m i_{mb} + N_b i_{sb1} = \frac{\phi_{a1}}{P_{a1}} + N_m i_{ma} + N_b i_{a1} \tag{6}$$

$$\frac{\phi_{b4}}{P_{b4}} - N_m i_{mb} - N_b i_{sb2} = \frac{\phi_{a1}}{P_{a1}} + N_m i_{ma} + N_b i_{a1} \tag{7}$$

According to that a sum of the magnetic fluxes is equal to zero, it can be written as,

$$\phi_{a1} + \phi_{a2} + \phi_{a3} + \phi_{a4} + \phi_{b1} + \phi_{b2} + \phi_{b3} + \phi_{b4} = 0 \tag{8}$$

$\varphi_{a1} \sim \varphi_{a4}$ and $\varphi_{b1} \sim \varphi_{b4}$ can be derived from (1)~(8).

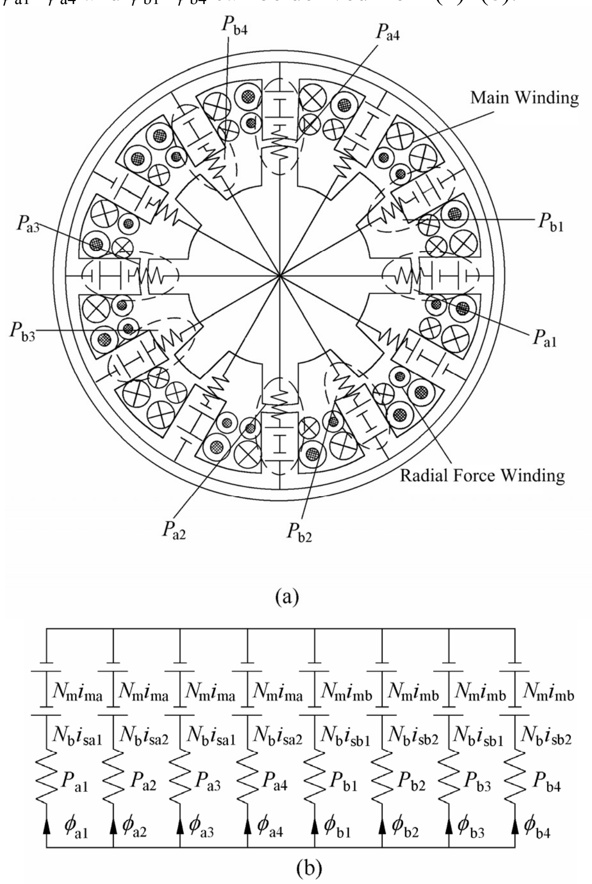

Fig. 1 Magnetic equivalent circuits

In order to calculate self and mutual inductances, it is required to obtain flux-linkages of each winding. The flux-linkage ψ_{ma} corresponding to motor winding current i_{ma} can be written from Fig. 1(a) as,

$$\psi_{ma} = N_m\left(-\phi_{a1} + \phi_{a2} - \phi_{a3} + \phi_{a4}\right) \tag{9}$$

Similarly, the flux-linkage ψ_{mb} corresponding to motor winding current i_{mb} and the flux-linkage of the radial force windings of phase A and B can be derived respectively.

Substituting $\varphi_{a1} \sim \varphi_{a4}$ and $\varphi_{b1} \sim \varphi_{b4}$ into the flux-linkages, and each phase's self and mutual inductances expressed by permeances can be derived from these formulas.

B. Permeance

If the rotor's radial displacement in the coordination of phase A is (α, β), it is ($\sqrt{3}\alpha/2 + \beta/2$, $\alpha/2 + \sqrt{3}\beta/2$) in the coordination of phase B. The rotational angle θ is defined as in Fig. 2.

The permeances P_{a1} and P_{b1} of the two-phase excitation mode can be derived as in [3].

$$P_{a1} = \frac{\mu_0 h r \theta (l_0 + \alpha)}{l_0^2} + \frac{2\mu_0 h}{\pi(\pi a - 2)} \times \left\{ \begin{aligned} & \pi a \ln\left(\frac{r(\pi - 12\theta)(l_0 + \alpha) + 12 a l_0^2}{12 a l_0^2}\right) \\ & + (\pi a - 4)\ln\left(\frac{\pi r(\pi - 12\theta)(l_0 + \alpha) + 24 l_0^2}{24 l_0^2}\right) \end{aligned} \right\} \tag{10}$$

$$P_{b1} = \frac{\mu_0 h r(\pi - 12\theta)\left(2l_0 + \sqrt{3}\alpha + \beta\right)}{24 l_0^2} + \frac{2\mu_0 h}{\pi(\pi a - 2)} \times \left\{ \begin{aligned} & \pi a \ln\left(\frac{r\theta\left(2l_0 + \sqrt{3}\alpha + \beta\right) + 2 a l_0^2}{2 a l_0^2}\right) \\ & + (\pi a - 4)\ln\left(\frac{\pi r\theta\left(2l_0 + \sqrt{3}\alpha + \beta\right) + 4 l_0^2}{4 l_0^2}\right) \end{aligned} \right\} \tag{11}$$

The $P_{a2} \sim P_{a4}$ and $P_{b2} \sim P_{b4}$ can be obtained similarly. There, $0 \le \theta \le \pi/12$.

μ_0—— permeability in the air

h—— stack length

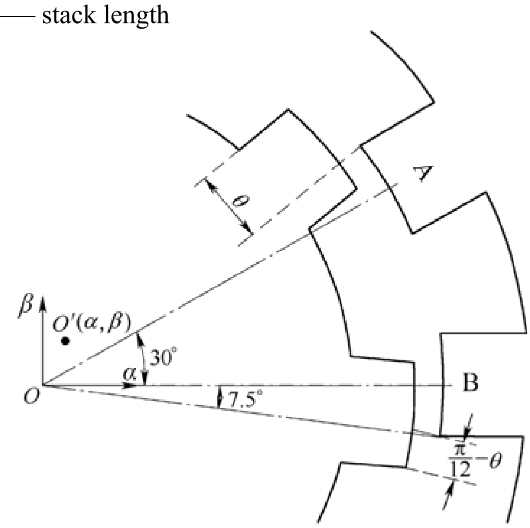

Fig. 2 Position of stator and rotor in two-phase state

r—— radius of rotor pole
l_0—— average air-gap length
a—— a constant of 1.01

Therefore, the formulas of self and mutual inductances can be derived.

C. Radial Force and Electromagnetic Torque

After the inductance matrix being built, the radial forces and the electromagnetic torque of BSRM with two-phase excitation are derived by the theory of virtual work.

$$\begin{bmatrix} F_\alpha \\ F_\beta \end{bmatrix} = \begin{bmatrix} \dfrac{\partial W}{\partial \alpha} \\ \dfrac{\partial W}{\partial \beta} \end{bmatrix} \approx i_{\mathrm{ma}} \begin{bmatrix} K_{\mathrm{f1}} & 0 \\ 0 & K_{\mathrm{f1}} \end{bmatrix} \begin{bmatrix} i_{\mathrm{sa1}} \\ i_{\mathrm{sa2}} \end{bmatrix} + i_{\mathrm{mb}} \begin{bmatrix} \sqrt{3}K_{\mathrm{f2}} & K_{\mathrm{f2}} \\ K_{\mathrm{f2}} & -\sqrt{3}K_{\mathrm{f2}} \end{bmatrix} \begin{bmatrix} i_{\mathrm{sb1}} \\ i_{\mathrm{sb2}} \end{bmatrix} \qquad (12)$$

Where,

$$K_{\mathrm{f1}} = N_{\mathrm{m}} N_{\mathrm{b}} \left\{ \frac{2\mu_0 h r \theta}{l_0^2} + \frac{4\mu_0 h}{\pi(\pi a - 2)} \times \left[\frac{\pi a r(\pi - 12\theta)}{r(\pi - 12\theta) l_0 + 12 a l_0^2} + \frac{\pi r(\pi a - 4)(\pi - 12\theta)}{\pi r(\pi - 12\theta) l_0 + 24 l_0^2} \right] \right\}$$

$$K_{\mathrm{f2}} = -N_{\mathrm{m}} N_{\mathrm{b}} \left\{ \frac{\mu_0 h r(\pi - 12\theta)}{12 l_0^2} + \frac{2\mu_0 h}{\pi(\pi a - 2)} \times \left[\frac{\pi a r \theta}{r\theta l_0 + a l_0^2} + \frac{\pi r(\pi a - 4)\theta}{\pi r \theta l_0 + 2 l_0^2} \right] \right\}$$

The instantaneous torque can be written as,

$$T = \frac{\partial W}{\partial \theta} \approx G_{\mathrm{t}}\left(\frac{\pi}{12} - \theta\right) \left(N_{\mathrm{m}}^2 i_{\mathrm{ma}}^2 + \frac{1}{2} N_{\mathrm{b}}^2 i_{\mathrm{sa1}}^2 + \frac{1}{2} N_{\mathrm{b}}^2 i_{\mathrm{sa2}}^2 \right) - G_{\mathrm{t}}(\theta) \left(N_{\mathrm{m}}^2 i_{\mathrm{mb}}^2 + \frac{1}{2} N_{\mathrm{b}}^2 i_{\mathrm{sb1}}^2 + \frac{1}{2} N_{\mathrm{b}}^2 i_{\mathrm{sb2}}^2 \right)$$

(13)

Where,

$$G_{\mathrm{t}}(\theta) = \frac{2\mu_0 h r}{l_0} - \frac{4\mu_0 h}{\pi(\pi a - 2)} \left[\frac{\pi a r}{a l_0 + r\theta} + \frac{\pi(\pi a - 4) r}{\pi r \theta + 2 l_0} \right]$$

III. OPERATING AREA

If phase A and B are turn-on all the time when θ varies from zero degree to fifteen, the average torque T_{avg} in two-phase excitation mode can be written as,

$$T_{\mathrm{avg}} = \frac{1}{\pi/12} \int_{\theta_{\mathrm{on}}}^{\theta_{\mathrm{off}}} T \mathrm{d}\theta = J_{\mathrm{t}} * \left[N_{\mathrm{m}}^2 \left(i_{\mathrm{ma}}^2 - i_{\mathrm{mb}}^2 \right) + \frac{1}{2} N_{\mathrm{b}}^2 \left(i_{\mathrm{sa1}}^2 + i_{\mathrm{sa2}}^2 - i_{\mathrm{sb1}}^2 - i_{\mathrm{sb2}}^2 \right) \right]$$

(14)

Where, T is the instantaneous torque,

$$J_{\mathrm{t}} = \frac{12}{\pi} \left\{ \frac{\pi \mu_0 h r}{6 l_0} - \frac{4\mu_0 h}{\pi(\pi a - 2)} \left[\pi a \ln\left(1 + \frac{\pi r}{12 a l_0}\right) - (\pi - 4) \ln\left(1 + \frac{\pi^2 r}{24 l_0}\right) \right] \right.$$

Fig. 3 shows the operating areas of BSRM in single and two-phase excitation modes. The operating area "OABC" is in the single-phase excitation mode while "OABD" is in the two-phase. The hatched section "BCD" represents the enlarged operating area. The maximum radial force enlarged 78% while the maximum torque keeps unvaried. The operating area of BSRM can be expanded to a great extent in the two-phase excitation mode. Therefore, there would be large enough radial force to keep the rotor levitating stably as the rotor pole deviates from the stator pole.

IV. VERIFICATION AND COMPARISON

The theoretical formulas of radial forces and instantaneous torque are verified with ANSYS. The simulation parameters of a test motor are shown in Table I.

Fig. 4 shows the curves of radial forces and instantaneous torque changing along with the rotational angle θ (i_{ma}=6A, i_{sa1}=i_{sa2}=4A, i_{mb}=8A, i_{sb1}=i_{sb2}=6A). The magnitude F of a vector composed of the instantaneous radial forces F_α and F_β can be written as, $F = \sqrt{F_\alpha^2 + F_\beta^2}$. It is seen that the theoretical values calculated in Fig. 4 are very close to simulation values. It is evident that the new theoretical formula from the simple magnetic equivalent circuit is effective.

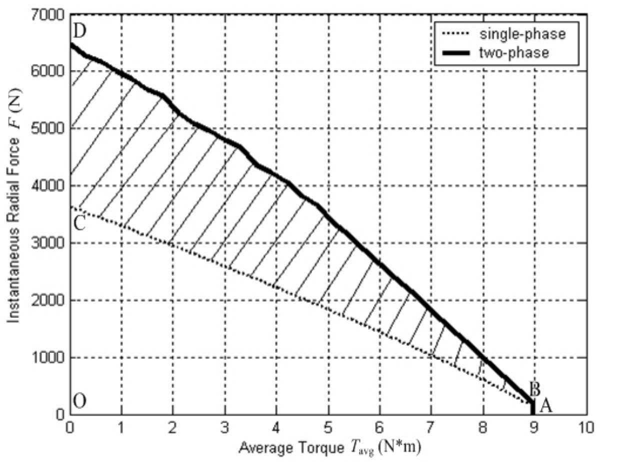

Fig. 3 Comparison of operating areas of single-phase mode and two-phase mode

TABLE I
SIMULATION PARAMETERS OF THE TEST MOTOR

Number of turns of motor main winding	22 turns
Number of turns of motor radial force winding	18 turns
Arc angle of rotor and stator teeth	15 degree
Outside diameter of stator core	145 mm
Inside diameter of stator pole	77 mm
Average air-gap length	0.25 mm
Inner diameter of rotor	30 mm
Radius of rotor pole	38.25 mm
Stack length	95 mm

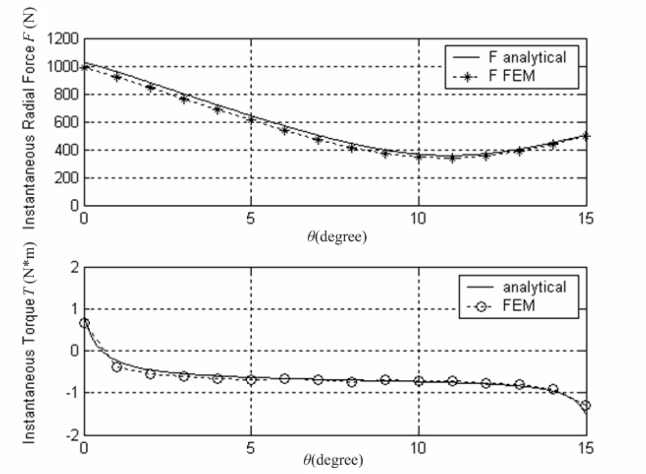

Fig. 4 Comparison of FEM results and analytical results

Fig. 5 shows the comparison of single-phase and two-phase mode (i_{ma}=i_{mb}=21A, i_{sa1}=i_{sa2}=14A, i_{sb1}=−14A, i_{sb2}=14A). It is seen that the radial forces become smaller and smaller when θ decreases in the single-phase mode. But in the two-phase mode, there are provided quite large radial forces in the whole period.

In 12/8 switched reluctance motors, there is always one phase generating negative torque in two-phase excitation mode. The torque generated in two-phase excitation mode is less than that in single-phase mode. Therefore each phase currents should be optimized to reduce the negative torque. Fig.6 shows the comparisons of optimized radial forces and torque in two-phase excitation mode and that in single-phase excitation mode.

In the first optimizing method, the main winding and radial force winding currents of phase A keep at the rated point while that of phase B vary linearly from the rated point to zero with θ varying from zero to fifteen degree. In the second optimizing method, the optimized currents are the same as in the first optimizing method when $\theta \geq 7.5$degree. When $\theta<7.5$degree, radial forces are kept the same as the value in $\theta=7.5$degree. The optimal currents can be found to insure that the generated torque keeps maximum. These two optimizing methods maintain the advantage of two-phase excitation that the radial forces increased. And the negative torque region is avoided. These two methods indicate different thoughts. They can be transformed considering different torque loads and radial loads in practice.

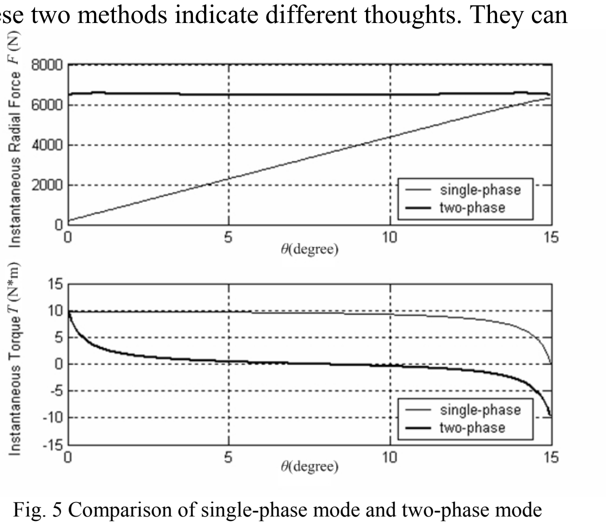

Fig. 5 Comparison of single-phase mode and two-phase mode

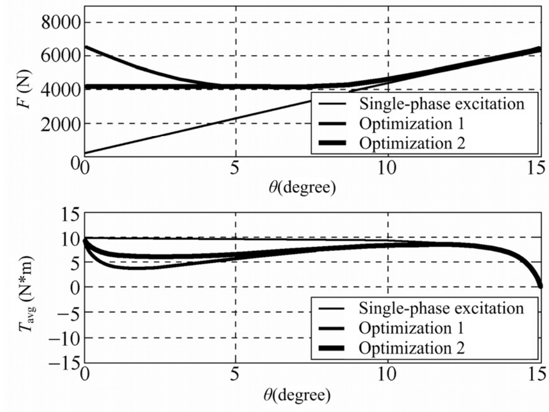

Fig. 6 Comparison of single-phase mode and optimal two-phase mode

Radial force becomes the major element in generating state. The sufficient radial forces should be produced primarily. It also needs to optimize the main winding and radial force winding currents. If i_{mb}=0 and i_{sb1}=i_{sb2}=0, the new mathematical model with two-phase excitation becomes the single-phase model. So the new model is flexible to both of single-phase and two-phase excitation mode.

V. CONCLUSIONS

This paper proposed a novel mathematical model of BSRM with two phases of main windings turn-on. First, the new model could be applied in both of single-phase and two-phase excitation. Second, the two-phase excitation mode brodened the operating area. Third, the two-phase excitation mode avoided the middle voltage's excurtion of the three-phase half-bridge converter applied in the radial force windings.

Therefore, this mathematical model solved the control problem of BSRM with two-phase excitation. The validity and fine characteristics of this mathematical model were verified by FEM.

REFERENCES

[1] Deng Zhiquan, Yang Gang, Zhang Yuan *et al*. "An innovative mathematical model for a bearingless switched reluctance motor". Proceedings of the CSEE, 2005, 25(9): 139-146

[2] Takemoto M, Shimada K, Chiba A *et al*. "A design and characteristics of switched reluctance type bearingless motors". NASA/CP-1998-207654, May 1998, pp49-63.

[3] Takemoto M, Chiba A, Akagi H *et al*. "Radial force and torque of a bearingless switched reluctance motor operating in a region of magnetic saturation". IEEE Trans. Industry Application, 2004, 40(1):104-112.

[4] Takemoto M, Suzuki H, Chiba A *et al*. "Improved analysis of a bearingless switched reluctance motor". IEEE Trans. Industry Application, 2001, 37 (1):26-34.

[5] Takemoto M, Chiba A, Fukao T. A new control method of bearingless switched reluctance motors using square-wave currents. Proceedings of the 2000 IEEE Power Engineering Society Winter Meeting, CD-ROM, January 2000: 375～380.

[6] Takemoto M, Chiba A, Fukao T. A method of determining the advanced angle of square-wave currents in a bearingless switched reluctance motor. IEEE Trans. Industry Application, 2001, 37(6): 1702～1709.